

Astrocyte Subtype Vulnerability in Stem Cell Models of Vanishing White Matter

Prisca S. Leferink, PhD ^{1†} Stephanie Dooves, MSc ^{1†} Anne E. J. Hillen, MSc,^{1†}
 Kyoko Watanabe, MSc,² Gerbren Jacobs, BSc,¹ Lisa Gasparotto, MSc,¹
 Paulien Cornelissen-Steijger, BSc,¹ Marjo S. van der Knaap, MD, PhD,^{1,3} and
 Vivi M. Heine, PhD ^{1,2}

Objective: Astrocytes have gained attention as important players in neurological disease. In line with their heterogeneous character, defects in specific astrocyte subtypes have been identified. Leukodystrophy vanishing white matter (VWM) shows selective vulnerability in white matter astrocytes, but the underlying mechanisms remain unclear. Induced pluripotent stem cell technology is being extensively explored in studies of pathophysiology and regenerative medicine. However, models for distinct astrocyte subtypes for VWM are lacking, thereby hampering identification of disease-specific pathways.

Methods: Here, we characterize human and mouse pluripotent stem cell-derived gray and white matter astrocyte subtypes to generate an in vitro VWM model. We examined morphology and functionality, and used coculture methods, high-content microscopy, and RNA sequencing to study VWM cultures.

Results: We found intrinsic vulnerability in specific astrocyte subpopulations in VWM. When comparing VWM and control cultures, white matter-like astrocytes inhibited oligodendrocyte maturation, and showed affected pathways in both human and mouse cultures, involving the immune system and extracellular matrix. Interestingly, human white matter-like astrocytes presented additional, human-specific disease mechanisms, such as neuronal and mitochondrial functioning.

Interpretation: Astrocyte subtype cultures revealed disease-specific pathways in VWM. Cross-validation of human- and mouse-derived protocols identified human-specific disease aspects. This study provides new insights into VWM disease mechanisms, which helps the development of in vivo regenerative applications, and we further present strategies to study astrocyte subtype vulnerability in neurological disease.

ANN NEUROL 2019;86:780–792

Astrocytes are increasingly recognized to play a role in the pathophysiology of different neurological diseases and suggested as the target in new therapies.^{1,2} Astrocytes consist of functionally and morphologically heterogeneous populations of cells that develop at different times and different locations in the central nervous system.^{3,4} Defects in specific astrocyte subtypes are shown in different neurological disorders,^{1,2} including epilepsy,⁵ amyotrophic lateral

sclerosis,⁶ Alzheimer disease,⁷ and vanishing white matter (VWM).⁸ VWM is one of the more prevalent leukodystrophies, caused by mutations in *EIF2B1–5*,⁹ and specific astrocyte subpopulations, like the astrocytes of the white matter, are affected.^{8,10,11} This vulnerability in astrocyte subtypes needs to be taken into consideration to better understand pathophysiology and to develop more targeted treatment options. Mouse studies have advanced our

View this article online at wileyonlinelibrary.com. DOI: 10.1002/ana.25585

Received Feb 13, 2019, and in revised form Jul 25, 2019. Accepted for publication Aug 18, 2019.

Address correspondence to Dr Heine, De Boelelaan 1085, 1081 HV Amsterdam, the Netherlands. E-mail: vm.heine@vumc.nl

[†]P.S.L., S.D., and A.E.J.H. share first authorship.

From the ¹Department of Pediatric Neurology, Emma Children's Hospital, Amsterdam UMC, Vrije Universiteit Amsterdam, Amsterdam Neuroscience, Amsterdam, the Netherlands; ²Department of Complex Trait Genetics, Center for Neurogenomics and Cognitive Research, Amsterdam Neuroscience, Vrije Universiteit Amsterdam, Amsterdam, the Netherlands; and ³Department of Functional Genomics, Center for Neurogenomics and Cognitive Research, Amsterdam Neuroscience, Vrije Universiteit Amsterdam, Amsterdam, the Netherlands

Additional supporting information can be found in the online version of this article.

knowledge on gene function in neural cell development,¹² and provide robust and standardized protocols, but do not always recapitulate the cellular or clinical phenotypes of human patients. The discovery of human induced pluripotent stem cells (hiPSCs) greatly enhanced the possibility to study neural disorders with patient-specific cells,¹³ but we still lack models to study phenotypes in specific neural subtypes. To identify disease mechanisms for a disorder like VWM, we are in need of iPSC differentiation protocols generating specific astrocyte subtypes.

In this study, we created in vitro models for VWM using hiPSCs and mouse induced pluripotent stem cells (miPSCs; Fig 1). We generated VWM- and control iPSC-derived astrocyte subtypes, using signaling molecules stimulating gray (using fetal bovine serum [FBS]) and white (including ciliary neurotrophic factor [CNTF]) matter. Interestingly, both hiPSC- and miPSC-derived white matter-like astrocytes showed specific vulnerability to VWM mutations. RNA sequencing (RNAseq) analysis

on hiPSC-derived white matter-like astrocytes indicated differential gene expression in VWM compared to control astrocytes involved in several cellular mechanisms, including neuronal, mitochondrial, and vasculature-related functioning. Of these pathways, genes involved in the immune system, cell development, and extracellular matrix also came up in miPSC-derived models, demonstrating the strength of cross-species validation in finding disease mechanisms induced by monogenic changes. These new insights can help development of more cell- or pathway-targeted therapies in VWM and other astrocyte-associated diseases.

Materials and Methods

hiPSC Differentiation toward Astrocytes

The institutional review board of Amsterdam UMC, Vrije Universiteit Amsterdam approved this study with waiver of informed consent. hiPSCs were generated from fibroblasts of 2 VWM patients with *EIF2B5* mutations (one 3-year-old male

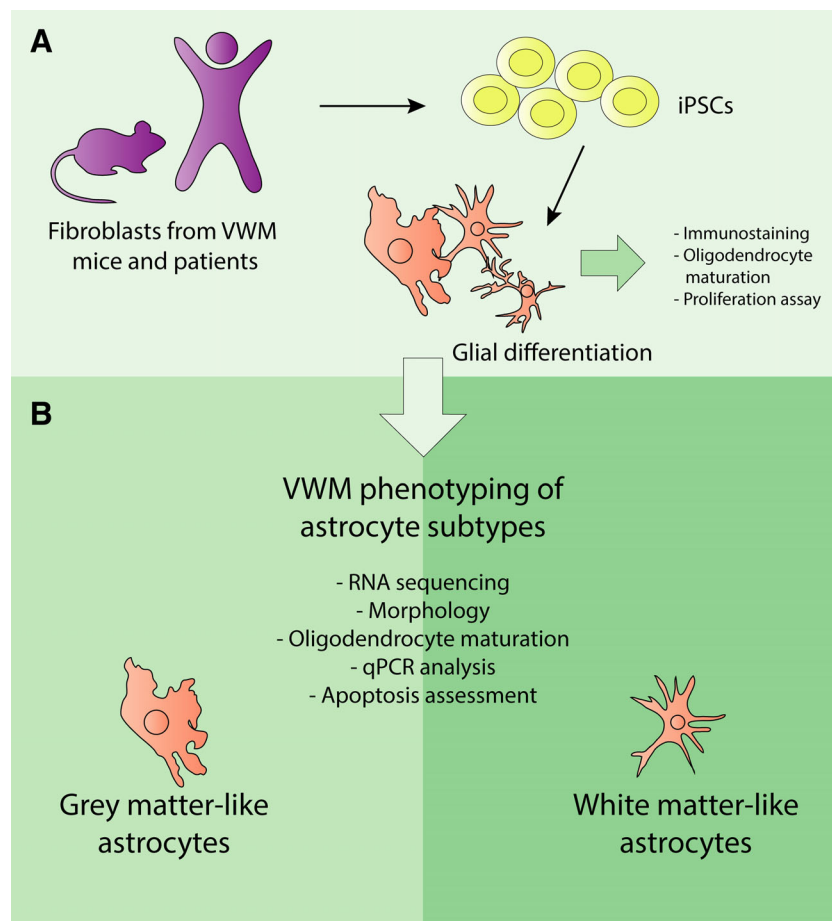


FIGURE 1: Experimental overview. (A) Fibroblasts from human and mouse, both vanishing white matter (VWM) genotype and control/wild type, were reprogrammed to induced pluripotent stem cells (iPSCs), and differentiated to glial cells for various assays. (B) The iPSCs were further differentiated to mouse and human gray matter and white matter astrocyte subtypes. The different astrocyte subtypes were used as an in vitro model for VWM, in which oligodendrocyte maturation and apoptosis, morphology, proliferation rate, and mRNA expression were studied. qPCR = quantitative polymerase chain reaction.

with 1484A>G mutation; one 9-year-old female with 806G>A mutation,) and 3 controls (males of 44, 46, and 74 days old) using a polycistronic lentiviral transduction of the Yamanaka factors.¹⁴ Cells were maintained and characterized as previously described,¹⁵ by alkaline phosphatase staining, immunocytochemistry, real-time polymerase chain reaction (RT-PCR) analysis, RNAseq PluriTest, and germ layer embryoid body (EB) differentiation assay, and karyotyped or tested on the Infinium Global Screening Array for DNA abnormalities. hiPSCs were differentiated toward human astrocytes as described previously.¹⁵ To generate human astrocyte subtypes, glial precursors were generated as described previously,¹⁵ after which medium was switched to N2B27-vitA medium supplemented with either epidermal growth factor (20ng/ml), fibroblast growth factor 2 (FGF2; 20ng/ml), and CNTF (20ng/ml) for human white matter–like astrocytes (human WM astrocytes), or with 10% FBS for human gray matter–like astrocytes (human GM astrocytes) for another 2 passages in 15 days. All differentiations are performed at least 3 times per iPSC clone, with at least 2 iPSC clones per donor.

miPSC Differentiation toward Glial Cells and Astrocytes

miPSCs from wild-type (wt), *Eif2b5*^{Arg191His/Arg191His} (*2b5*^{ho}), and *Eif2b4*^{Arg484Trp/Arg484Trp}*Eif2b5*^{Arg191His/Arg191His} (*2b4*^{ho}*2b5*^{ho}) mice were made from fibroblasts with viral transduction of the Yamanaka factors.¹⁴ Cells were maintained in 2i medium on gelatin-coated plates. miPSCs were characterized by using immunocytochemistry, PCR analysis, EB differentiation assay, and teratoma formation assay. miPSCs were differentiated via EB formation in basal medium followed by neural induction in N2-based medium supplemented with retinoic acid (0.2μM) and purmorphamine (1μM). After 8 days, EBs were plated in neural maintenance medium (N2-based) supplemented with 20ng/ml FGF2 for 12 days.

For glial differentiation, the glial progenitor cells were subsequently cultured in mouse neural maintenance medium supplemented with 30ng/ml T3 and 10ng/ml NT3 from day 12 on. At day 18, cells were used for analysis. For mouse astrocyte subtypes cells were cultured in mouse neural maintenance medium supplemented with 10% FBS for mouse gray matter–like astrocytes (mouse GM astrocytes) or 10ng/ml CNTF for mouse white matter–like astrocytes (mouse WM astrocytes) from day 12 onward. To obtain purer astrocyte cultures, cells were passed every 7 days for an additional 2 passages. At day 32, cells were used for analysis. All immunostaining and PCR analysis of miPSC-derived cells are an average of at least 3 independent differentiations and based on 3 to 4 iPSC lines per genotype.

Isolation and Culture of Primary Cells

Primary astrocytes and oligodendrocyte precursor cells were isolated from forebrain of embryonic day 18 mice as described previously.¹⁰ Oligodendrocyte precursor cells were sorted on expression of platelet-derived growth factor receptor α with magnetically activated cell sorting according to the manufacturer's protocol (Miltenyi Biotec, Bergisch Gladbach, Germany).¹⁰

Analysis

Cells were analyzed by immunocytochemistry as previously described.¹⁵ Primary antibodies targeted glial fibrillary acidic protein (GFAP; Sigma, St Louis, MO; G3893, 1:1,000), GFAP (Dako, Carpinteria, CA; Z0334, 1:1,000), nestin (BD Biosciences, Franklin Lakes, NJ; 611658, 1:500), S100 β (Proteintech Group, Rosemont, IL; 15146-1-AP, 1:1,000), Olig2 (for mouse, gift of J. H. Alberta, 1:500), Olig2 (for human, Millipore, Billerica, MA; AB9610, 1:500), Sox9 (Cell Signaling Technology, Danvers, MA; 82630, 1:500), myelin basic protein (MBP; Covance, Princeton, NJ; SMI-99P, 1:2,000), CD44 (Developmental Studies Hybridoma Bank, Iowa City, IA; H4C4, 1:250), ID3 (Cell Signaling Technology, 9837, 1:250), ezrin (Santa Cruz Biotechnology, Santa Cruz, CA; sc-32759, 1:450), myelin oligodendrocyte glycoprotein (MOG; Millipore, MAB5680, 1:500), cleaved caspase 3 (Cell Signaling Technology, 9661, 1:400), OCT3/4 (Santa Cruz Biotechnology, sc-5279, 1:1,000), nanog (Abcam, Cambridge, MA; AB80892, 1:1,000), Lin28a (Cell Signaling Technology, 3978s, 1:1,000), β -tubulin-III (R&D Systems, Minneapolis, MN; MAB1195, 1:1,000), α -smooth muscle actin (Progen, Heidelberg, Germany, 61001, 1:1,000), α -fetoprotein (R&D Systems, MAB1368, 1:1,000), Tra-1-60 (Santa Cruz Biotechnology, sc-21705, 1:200), and SSEA4 (Developmental Studies Hybridoma Bank, [SSEA-4]-s, 1:50).

Bromodeoxyuridine (BrdU) assay was performed (2 independent differentiations of 4 human astrocyte lines per genotype) by 2-hour incubation of BrdU at 37°C and stained with anti-BrdU antibody (Abcam) according to the manufacturer's protocol. RNA was collected with TRIzol (Invitrogen, Carlsbad, CA). RNA isolation, cDNA synthesis, and PCR analysis were performed as described previously (see Supplementary Table 1 for primer sequences).¹⁵ Calcium imaging of glutamate uptake in human astrocytes was performed and analyzed as described previously.¹⁵ For reactivity assay, human astrocytes were treated with either 10μg/ml polyinosinic:polycytidylic acid (Tocris Bioscience, Bristol, UK) or dH₂O for 21 hours, after which RNA was isolated and analyzed as described previously.¹⁵

For RNAseq, an Illumina (San Diego, CA) TruSeq stranded mRNA kit was used according to the manufacturer's protocol. Sequence fragments were aligned to the reference genome (mouse: GRCm38, annotated genes GENCODE vM12; human: GRCh38, annotated genes GENCODE v25). Only genes on autosomal chromosomes were extracted, and all genes with a transcripts per kilobase million of <1 in 50% of samples were excluded. Differential expression analysis was performed using R package DESeq2. Genes with Bonferroni corrected $p < 0.05$ were considered significantly differentially expressed genes (DEGs) and used for gene-set enrichment analysis using Gene Ontology (GO) terms. For human samples, analysis was done with covariate factors, which included individual, the number of clones per individual, and the number of differentiation repetitions per clone.

Statistical Analysis

For all experiments, results were considered significant at $\alpha = 0.05$ after multiple test correction. Apart from the RNAseq data, all other data are analyzed with IBM (Armonk, NY) SPSS

statistics version 22 and Microsoft (Redmond, WA) Excel 2016. Shapiro–Wilk test was used to confirm normal distribution of data, and all data were tested with 2-tailed tests. *T* tests were used to compare FBS and CNTF astrocytes and VWM patients versus controls. To compare wt, $2b5^{ho}$, and $2b4^{ho}2b5^{ho}$ mouse data, 1-way analysis of variance with Dunnett post hoc tests was used.

Results

miPSC-Based Models Recapitulate Oligodendrocyte Precursor Cell Maturation Inhibition by VWM Astrocytes

Previous studies showed that astrocytes isolated from VWM mouse models impair primary oligodendrocyte precursor cell maturation via secreted factors, suggesting that astrocytes are the primary affected cell type in VWM.¹⁰ To show that iPSC-derived cell models recapitulate findings in primary cell models and to confirm that astrocytes cause cellular defects in VWM, we developed an in vitro miPSC model based on previous experiments with primary mouse cells. We generated miPSCs from wt, $2b5^{ho}$, and the severely affected $2b4^{ho}2b5^{ho}$ mice. The miPSCs were differentiated toward glia cultures containing both astrocytes (~15–25% GFAP-positive cells) and oligodendrocytes (~30–40% Olig2-positive cells; Fig 2). Similar to previous primary mouse studies, oligodendrocyte maturation was significantly impaired in VWM cultures, as was demonstrated by decreased ratios of MBP-/Olig2-positive cells in $2b4^{ho}2b5^{ho}$ cultures ($F_{2,6} = 14.24, p = 0.005$; post hoc Dunnett wt vs $2b4^{ho}2b5^{ho}, p = 0.039$) and MOG-/4,6-diamidino-2-phenylindole– (DAPI) positive cells in both $2b5^{ho}$ and $2b4^{ho}2b5^{ho}$ cultures ($F_{2,5} = 7.83, p = 0.029$; post hoc Dunnett wt vs $2b5^{ho}, p = 0.047$; wt vs $2b4^{ho}2b5^{ho}, p = 0.047$), whereas the percentage of Olig2-positive cells remained unchanged. To confirm that the decreased oligodendrocyte maturation was caused by astrocytes, we added healthy primary mouse astrocytes; wt mouse astrocytes rescued the oligodendrocyte maturation defect, demonstrating that miPSC models recapitulate cellular models using primary cells, and confirming previous findings that VWM astrocytes are responsible for oligodendrocyte maturation defects.

VWM Patient iPSC-Based Models Confirm Intrinsic Defects in VWM Astrocytes

To recapitulate findings with hiPSC models, we generated hiPSCs from VWM patients and healthy control donor fibroblasts. To generate astrocytes, we differentiated control and VWM hiPSCs toward astrocytes according to protocols described earlier.¹⁵ We characterized the human astrocytes for expression of the astrocyte-associated markers GFAP, nestin, Id3, CD44, and SOX9 by immunocytochemistry (Fig 3), and *NESTIN*, *BLBP*, *S100β*,

ALDOC, *AQP4*, *GLAST*, *GFAP*, and *CD44* by RT-PCR (data not shown). Functionality of human astrocytes was demonstrated using calcium imaging, showing glutamate uptake in both control and VWM lines (data not shown). To confirm increased proliferation in VWM astrocytes as was described earlier for primary human astrocytes,⁸ we performed a BrdU incorporation assay. The VWM astrocytes showed a significantly higher percentage of proliferating cells compared to control human astrocytes (independent $t_6 = 2.56, p = 0.042$). To show that human astrocytes can mediate an oligodendrocyte maturation defect via secretion of factors in media as suggested by mouse studies,¹⁰ primary mouse oligodendrocyte precursor cells were cultured in medium conditioned by control and patient iPSC-derived astrocytes. Media conditioned by VWM astrocytes significantly impaired oligodendrocyte maturation, as measured by the percentage of MBP-/Olig2-positive cells (independent $t_3 = 2.34, p = 0.049$). As hyaluronic acid has been previously described to inhibit oligodendrocyte maturation¹⁶ and is increased in brains of VWM patients,¹⁷ media conditioned by human astrocytes was treated with hyaluronidase. Hyaluronidase-treated conditioned medium significantly increased oligodendrocyte maturation in VWM cultures (independent $t_3 = -8.62, p = 0.002$), which recovered toward control levels. Altogether, our results demonstrate that hiPSC models recapitulate findings in both primary human cells and in miPSC cell models. Furthermore, we confirmed an astrocyte-intrinsic defect in VWM using hiPSC models.

miPSC-Based Models Show Selective Involvement of Astrocytic Subtypes in VWM

An increasing number of studies confirm heterogeneity among astrocytes, such as white and gray matter astrocytes. However, we lack iPSC-based differentiation protocols generating specific subtypes. CNTF and FBS are both used in astrocyte differentiation protocols.^{18,19} Where CNTF-reactive astrocytes are predominantly found in the white matter,²⁰ FBS administration is standardly used to maintain cortical astrocytes,²¹ leading to a flat morphology that is common for gray matter astrocytes in culture. Here we used CNTF- and FBS-based media to generate mouse WM astrocytes and mouse GM astrocytes, respectively. The mouse WM astrocytes had many thin protrusions, were smaller, and had higher expression of *Glast*, *S100b*, and *Gfap* (data not shown) compared to the larger and rounder mouse GM astrocytes (Fig 4). To assess functional defects in the 2 astrocyte subtypes in VWM, wt mouse primary oligodendrocyte precursor cells were cultured in media conditioned by mouse WM and GM astrocytes, derived from wt, $2b5^{ho}$, and $2b4^{ho}2b5^{ho}$ miPSCs. Oligodendrocyte maturation was not affected in conditioned

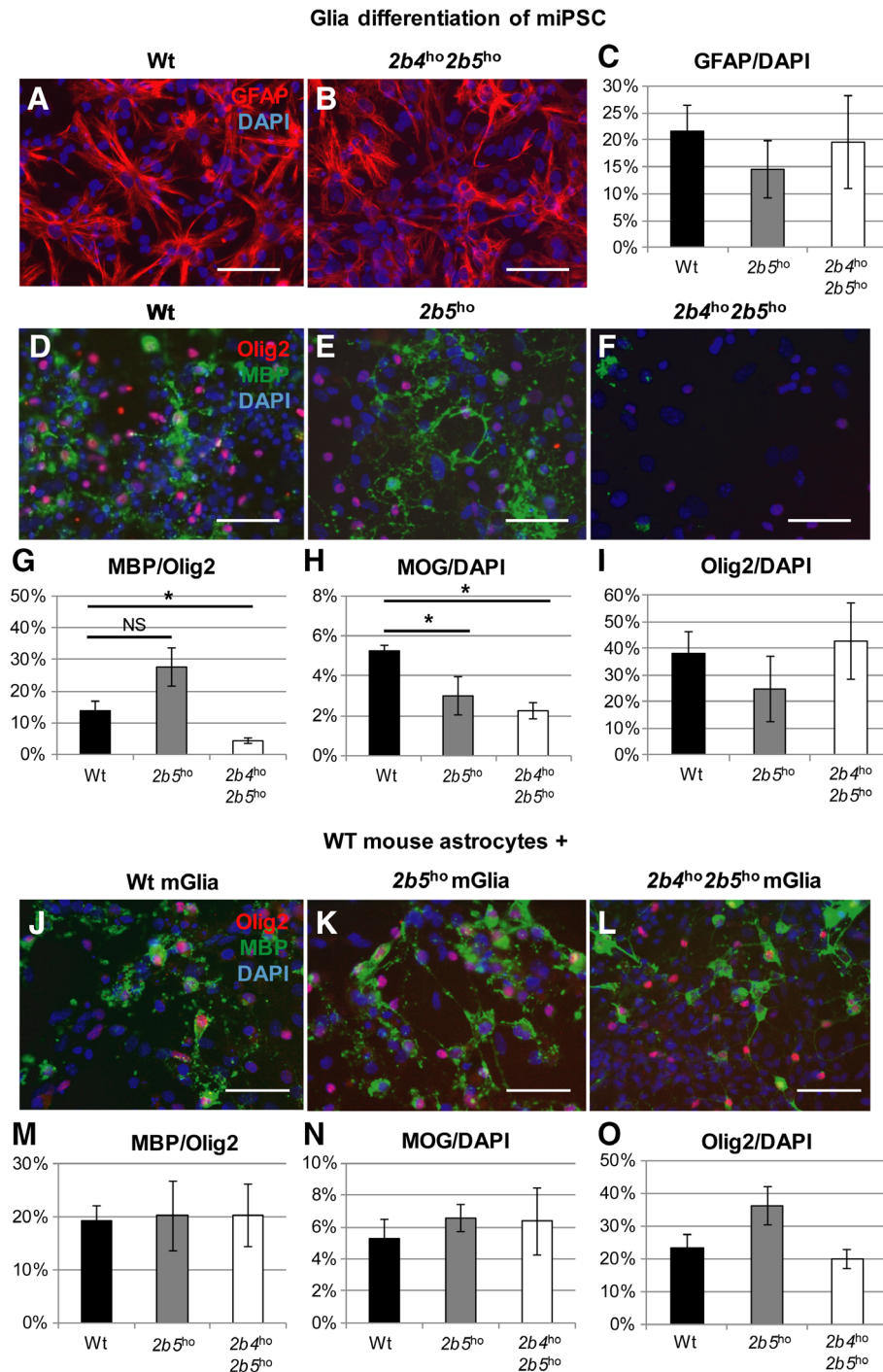


FIGURE 2: Wild-type (wt) astrocytes rescue the maturation defect of vanishing white matter (VWM) mouse induced pluripotent stem cell (miPSC)-derived oligodendrocytes. (A–C) Glial differentiation contained glial fibrillary acidic protein (GFAP)-positive astrocytes, as shown by immunocytochemistry (A, B) and quantification (C). (D–I) Oligodendrocyte maturation was addressed in wt, $2b5^{ho}$, and $2b4^{ho}2b5^{ho}$ glia by immunostaining for myelin basic protein (MBP), myelin oligodendrocyte glycoprotein (MOG), and Olig2. Cell counts confirmed the decrease in the number of MBP-positive (G) and MOG-positive cells (H) in VWM without a decrease in the number of Olig2⁺ cells (I). Percentages of positive cells compared to the number of Olig2-positive cells are shown for MBP; H and I show the percentage of total number of 4,6-diamidino-2-phenylindole (DAPI)-positive cells (wt, n = 3; $2b5^{ho}$, n = 3; $2b4^{ho}2b5^{ho}$, n = 3). (J–O) To investigate the effect of healthy astrocytes on the oligodendrocyte precursor cell maturation defect, wt, $2b5^{ho}$, and $2b4^{ho}2b5^{ho}$ glia were grown on a monolayer of wt primary mouse astrocytes, and oligodendrocyte maturation was assessed using an immunostaining for MBP, MOG and Olig2. The oligodendrocyte maturation was no longer reduced in VWM cultures, as demonstrated by the absence of significant differences in the MBP/Olig2 (M) and MOG/DAPI (N) ratios between wt, $2b5^{ho}$, and $2b4^{ho}2b5^{ho}$ cultures. The Olig2/DAPI ratio was slightly, but not significantly, increased in $2b5^{ho}$ cultures (O; wt, n = 3; $2b5^{ho}$, n = 3; $2b4^{ho}2b5^{ho}$, n = 4). Scale bars = 50 μ m. *Significant at p < 0.05. Bars in C, G–I, M–O represent mean \pm standard error of the mean. NS = not significant.

Astrocyte differentiation of hiPSC

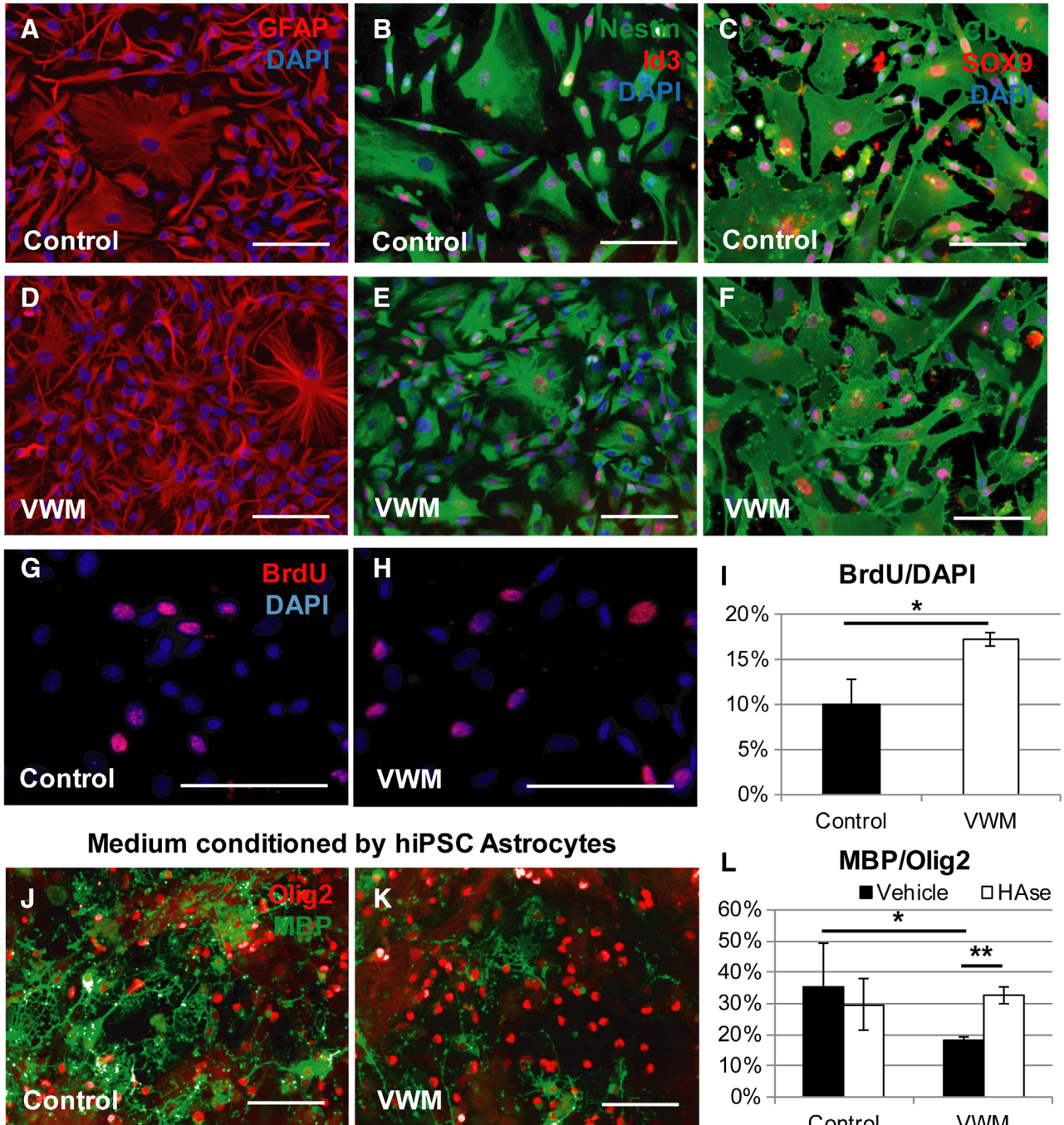


FIGURE 3: Human induced pluripotent stem cell (iPSC)-derived astrocytes confirm a cell-intrinsic vanishing white matter (VWM) phenotype. (A–F) Immunostaining showed expression of astrocyte markers glial fibrillary acidic protein (GFAP; A, D), nestin and Id3 (B, E), and CD44 and SOX9 (C, F) in both control (A–C) and VWM (D–F) human astrocyte cultures. To quantify proliferation of the astrocytes, bromodeoxyuridine (BrdU) labeling was performed. (G, H) Representative control (G) and VWM (H) astrocyte lines are shown. Quantification of proliferation was assessed using the percentage of BrdU-labeled cells of the total population of cells (4,6-diamidino-2-phenylindole [DAPI]) in control human iPSC (hiPSC)-derived astrocytes. (I) VWM astrocytes showed increased proliferation compared to control astrocytes. (J, K) Immunostaining for Olig2 and myelin basic protein (MBP) of primary wild-type embryonic day 18 mouse oligodendrocyte precursor cells cultured for 7 days in media conditioned by hiPSC-derived astrocytes in representative examples of VWM and control cultures is shown. Maturation of the oligodendrocyte precursor cells was assessed using a ratio of MBP-positive cells of the total Olig2-positive population, in the presence of media conditioned by control and VWM iPSC-derived astrocytes. Astrocyte conditioned media were treated with either vehicle or hyaluronidase (HAse). (L) Oligodendrocyte maturation was impaired in VWM compared to control cultures, and HAse rescued oligodendrocyte maturation comparable to control level. Scale bars = 100µm. *p < 0.05, **p < 0.01.

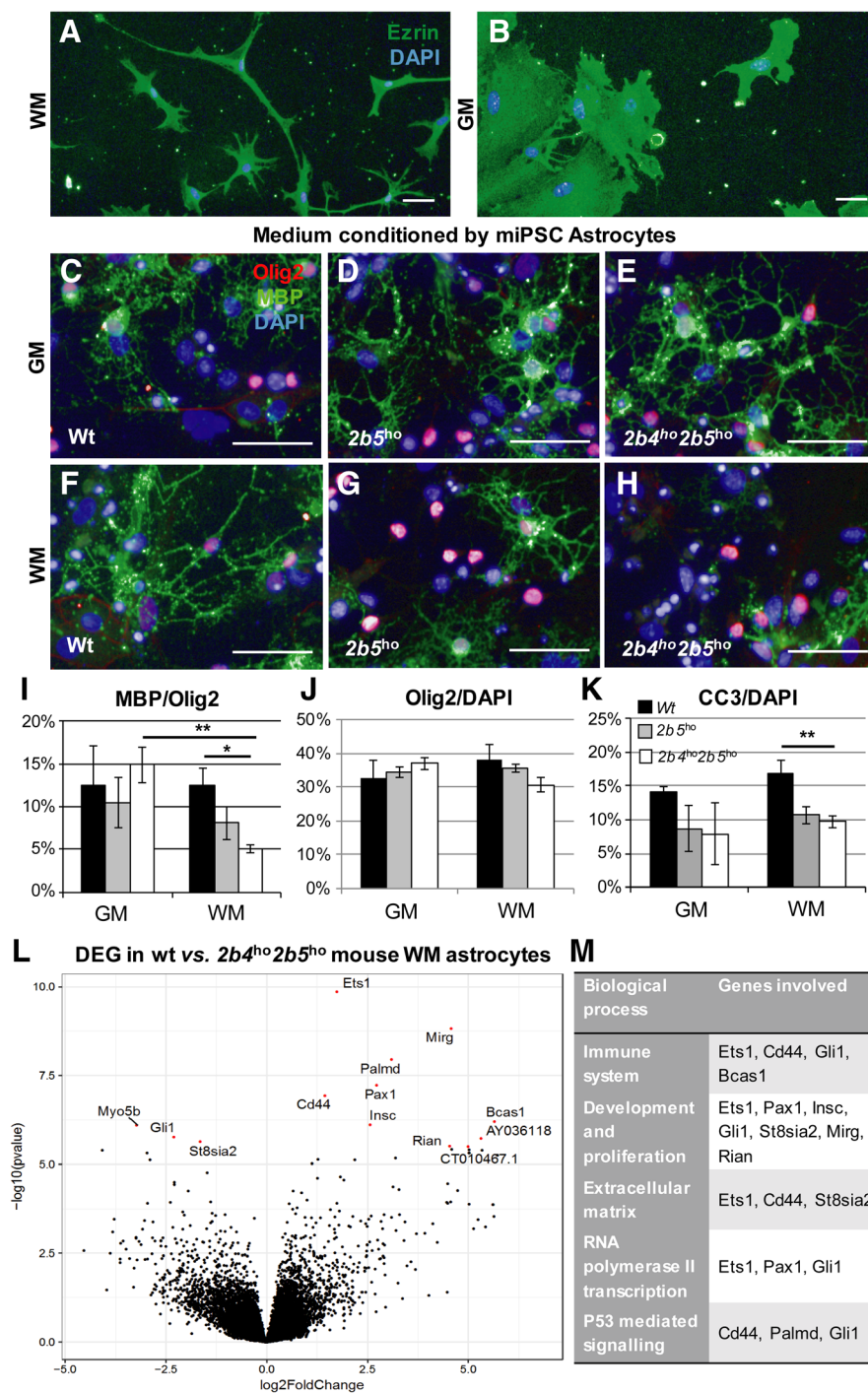


FIGURE 4: Mouse white matter (WM) and gray matter (GM) astrocytes are differentially affected by vanishing white matter (VWM) mutation. (A, B) Immunostaining for cytoplasmic cell surface marker ezrin of mouse induced pluripotent stem cell (miPSC)-derived WM (A) and GM astrocytes (B) showed morphological differences between the cells. (C–H) To assess functional defects of VWM mouse WM and GM astrocytes, wild-type (wt) mouse primary oligodendrocyte precursor cells were cultured in conditioned medium collected from wt (n = 3), 2b5^{ho} (n = 4), and 2b4^{ho}2b5^{ho} (n = 4) iPSC-derived GM or WM astrocytes (respectively GM and WM in I–K). Oligodendrocyte maturation was quantified as the percentage of myelin basic protein (MBP)-positive oligodendrocytes of the number of Olig2-positive cells. (I, J) This percentage was significantly decreased in 2b4^{ho}2b5^{ho} GM medium compared to wt WM medium and 2b4^{ho}2b5^{ho} GM medium (I), whereas the percentage of Olig2-positive cells was unchanged between the conditions (J). To assess apoptosis in the oligodendrocyte cultures, a cleaved caspase 3 (CC3) assay was conducted in oligodendrocyte cultures with conditioned medium of GM and WM astrocytes of wt (n = 4), 2b5^{ho} (n = 4), and 2b4^{ho}2b5^{ho} (n = 4). (K) The percentage of CC3-positive cells of 4,6-diamidino-2-phenylindole (DAPI)-positive cells was significantly decreased in VWM compared to control WM cultures. *p < 0.05, **p < 0.01. Scale bars = 50µm. Bars in I–K represent mean ± standard error of the mean. (L) Volcano plot of differential expression analysis between wt (n = 4) and 2b4^{ho}2b5^{ho} (n = 4) mouse WM astrocytes with significant differentially expressed genes (DEGs). Significant DEGs are colored in red and are labeled. (M) Significantly enriched Gene Ontology terms for DEGs in different categories.

medium of VWM GM astrocytes. However, the mouse WM astrocyte conditioned medium from the $2b4^{ho}2b5^{ho}$ mutants significantly decreased the percentage of MBP-/Olig2-positive cells compared to mouse WM astrocyte conditioned medium from controls ($F_{2, 8} = 6.23$, $p = 0.023$; post hoc Dunnett wt vs $2b4^{ho}2b5^{ho}$, $p = 0.014$) and mouse GM astrocyte conditioned medium from $2b4^{ho}2b5^{ho}$ mutants ($t_3 = -6.111$, $p = 0.009$). The percentage of Olig2-positive cells was unchanged between conditions. In the cultures containing conditioned media of mouse WM astrocytes, the percentage of oligodendrocyte precursor cells positive for apoptotic marker cleaved caspase 3 was significantly reduced in the $2b5^{ho}$ and $2b4^{ho}2b5^{ho}$ mutants compared to controls ($F_{2, 9} = 9.231$, $p = 0.007$, post hoc Dunnett wt vs $2b5^{ho}$, $p = .014$; wt vs $2b4^{ho}2b5^{ho}$, $p = 0.006$). No significant differences in the percentage of cleaved caspase 3-positive cells were observed in the GM condition. Altogether, these findings demonstrate that mouse WM astrocytes show a higher vulnerability to VWM mutations.

Because mouse WM astrocytes are selectively affected by VWM mutations, we performed transcriptome analysis on *wt* and $2b4^{ho}2b5^{ho}$ cultures to identify DEGs in the affected astrocytes. Interestingly, only a selected number of genes were significantly affected by VWM mutations; in total, 13 genes were significantly differentially expressed between the *wt* and $2b4^{ho}2b5^{ho}$ WM astrocytes (Supplementary Table 2), as labeled in Figure 4L. Based on enrichment analysis for DEGs with GO terms and literature,^{22–25} DEGs were overrepresented in the categories “Immune System,” “Development and Proliferation,” “Extracellular Matrix,” “RNA Polymerase II Transcription,” and “P53 Mediated Signaling” (see Fig 4M), suggesting that these processes are differentially regulated between VWM and wt mouse WM astrocytes.

hiPSCs Differentiate into Distinctive Astrocytic Subpopulations

To show astrocyte subtype-specific abnormalities in human VWM cells, we used CNTF- and FBS-based media to generate human WM astrocytes and human GM astrocytes, respectively. Similar to mouse cultures, human WM astrocytes presented as smaller cells with many and thin protrusions compared to the rounder and larger human GM astrocytes (Fig 5A, B) and showed significantly increased expression in astrocyte markers including *SOX9*, *NESTIN*, and *BLBP* (data not shown). Both astrocyte subtypes showed appropriate upregulation of reactivity-related genes in response to cellular stressor polyinosinic:polycytidylic acid (data not shown), but no differences in reactive response were observed. As, to our knowledge, there are no transcriptome profiles of cultured, or purified, human gray

and white matter astrocytes, we performed whole-genome transcriptome analysis on our human WM and GM astrocyte subtypes. Figure 5C shows a volcano plot of DEGs in human WM compared to human GM astrocytes. In total, 346 genes were significantly differentially expressed between the subtypes (Supplementary Table 3). Enrichment analysis with GO terms (Molecular Functions) on the DEGs between human WM and GM astrocytes could be classified in the categories “Receptor/Ligand Activity,” “Extracellular Space,” “Enzymatic Activity,” “Immune System,” and “Cytoskeleton” (see Fig 5D). These findings show that we generated 2 human astrocyte subpopulations in vitro: human WM and GM astrocytes, with specific morphological characteristics and differential expression profiles.

VWM Mutations Predominantly Affect White over Gray Matter Astrocyte Subtype in hiPSC-Based Cultures

To perform unbiased differential expression analysis, we performed transcriptome analysis of VWM and control human WM astrocytes. In total, 63 genes were significantly differentially expressed between the VWM and controls (Supplementary Table 4). A volcano plot of covariate-corrected DEGs in VWM compared to controls is shown in Figure 6A. When comparing VWM and control human GM astrocytes, 37 DEGs were detected (Supplementary Table 5), which is almost half the number of DEGs found in the white matter subtype. A volcano plot presents the covariate-corrected DEGs in VWM compared to control human GM astrocytes in Figure 6B. Enrichment analysis of GO terms (Biological Processes) on the DEGs between control and VWM WM astrocytes could be categorized as “Immune System,” “Extracellular Space,” “Cell Development,” “Neuronal Functioning,” and “Vasculature-Related,” whereas the DEGs between control and VWM GM astrocytes did not show significant enrichment in the latter 2 categories (see Fig 6). Because these results demonstrate that the human WM astrocytes presented a more broadly modulated transcript profile by a VWM genotype than the human GM astrocytes, the differences in the human WM astrocyte cultures were further investigated. The VWM human WM astrocytes showed different morphologies compared to controls, although these did not reach statistical significance when quantified using automated Columbus software (PerkinElmer, Waltham, MA). The VWM cells were rounder (2-sample $t_4 = 0.62$, $p = 0.58$), showed a larger surface area (2-sample $t_4 = 1.78$, $p = 0.15$), and had a reduced perimeter corrected for the surface area (2-sample $t_4 = -1.00$, $p = 0.37$) compared to control cells. Furthermore, expression analysis for astrocyte-associated markers by quantitative PCR analysis showed that VWM

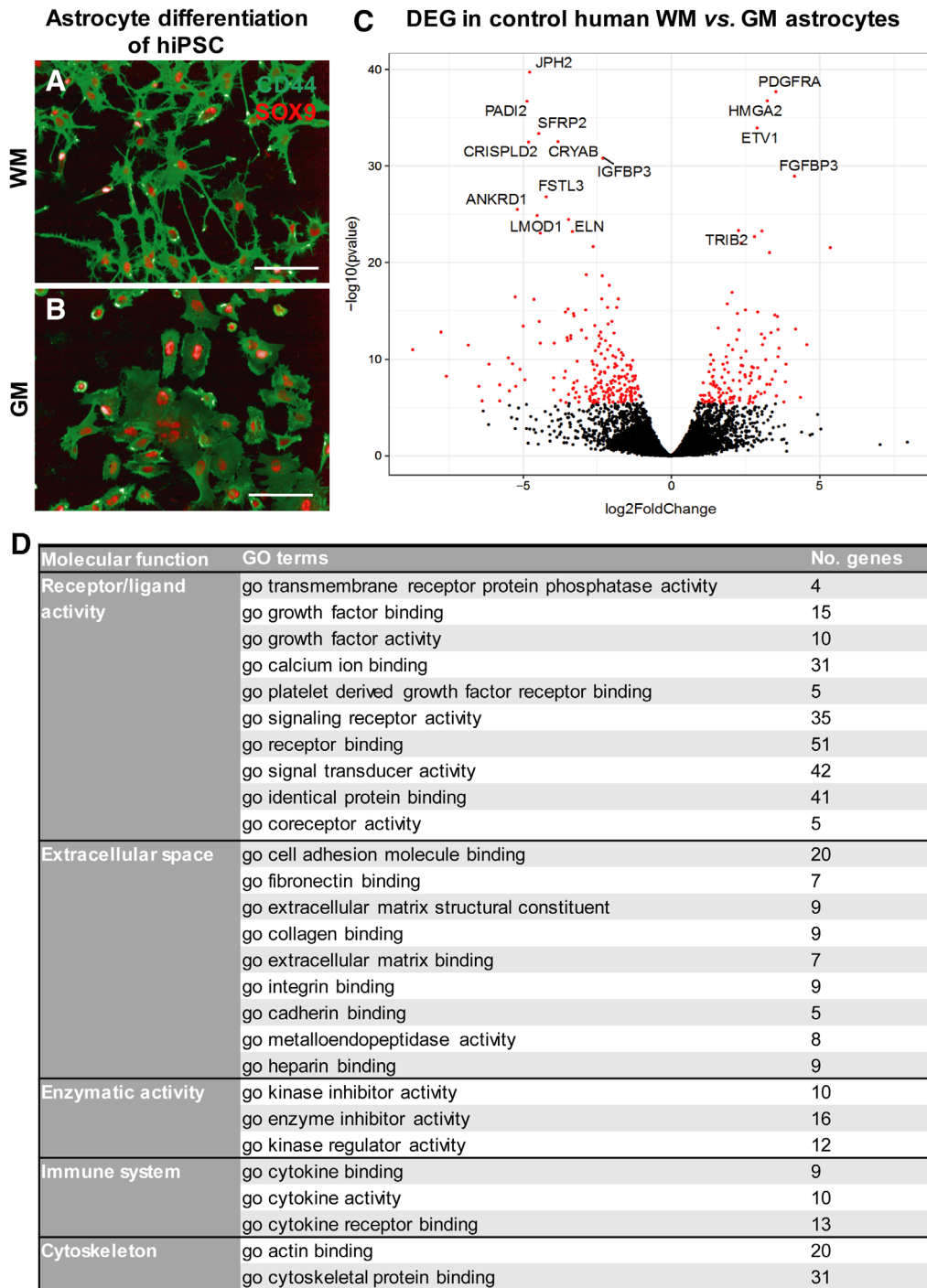


FIGURE 5: Human white matter (WM) and gray matter (GM) astrocyte subtypes differ in morphology and transcriptome. (A, B) Immunostaining showed expression of astrocyte markers CD44 and SOX9 in control human induced pluripotent stem cell (hiPSC)-derived WM (A) and GM astrocytes (B). Scale bars = 100µm. **(C)** Volcano plot of differential expression analysis of control human WM astrocytes and human GM astrocytes shows significant differentially expressed genes (DEGs) in red. The 15 most significantly up- or downregulated DEGs are labeled. **(D)** Significantly enriched Gene Ontology (GO) terms per molecular function classified the DEGs into different categories.

human WM astrocytes had a significantly higher expression of *AQP4* (2-sample $t_5 = 2.94$, $p = 0.032$) and *NESTIN* (2-sample $t_5 = 3.61$, $p = 0.015$). There was no difference in the expression of cleaved caspase 3 in oligodendrocyte precursor cells that were cultured in medium

conditioned by VWM or control human WM astrocytes, or for human GM astrocyte conditioned media. Together, these findings demonstrate that human WM astrocytes were more profoundly affected by the VWM genotype than human GM astrocytes.

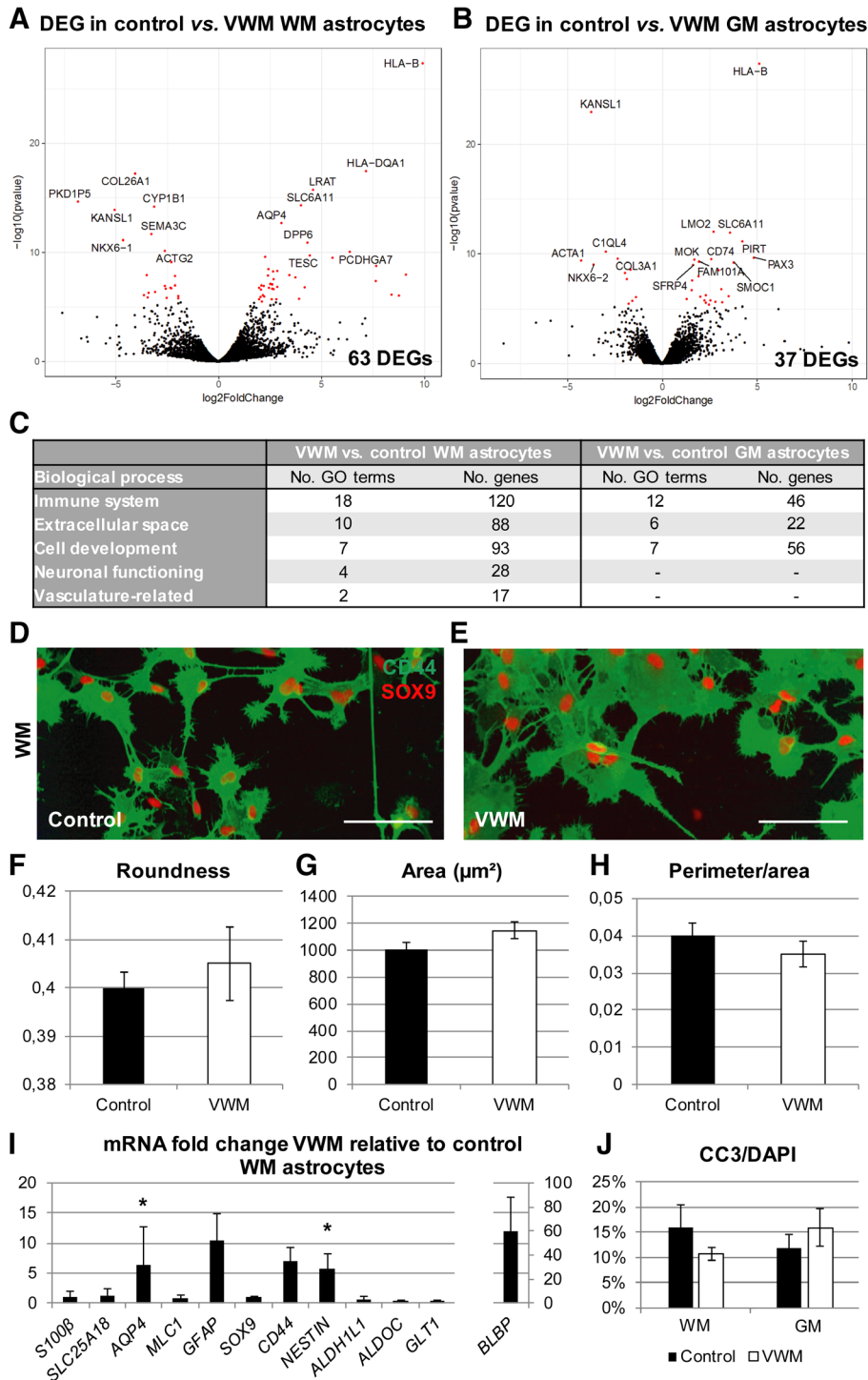


FIGURE 6: Vanishing white matter (VWM) human astrocyte subtypes differ in morphology and mRNA expression level from control human astrocyte subtypes. (A, B) Differential expression analysis revealed significant differentially expressed genes (DEGs) between VWM and control in human white matter (WM) astrocytes (A; control, n = 3; VWM, n = 4) and human gray matter (GM) astrocytes (B; control, n = 4; VWM, n = 4). The volcano plots indicate significant DEGs in red, with the 15 most significantly up- or downregulated DEGs labeled. **(C)** Significantly enriched Gene Ontology (GO) terms classified the DEGs in different categories of biological processes. **(D, E)** Morphology of control (D) and VWM (E) human WM astrocytes was visualized using CD44 and SOX9 immunostaining. **(F–H)** Morphological analysis showed differences in roundness (F), area (G), and perimeter corrected for area (H) between VWM and control human WM astrocytes based on the CD44 immunostaining. **(I)** A quantitative polymerase chain reaction on VWM human WM astrocytes (n = 4) showed differential expression of *S100B*, *SLC25A18*, *MLC1*, *SOX9*, *CD44*, *NESTIN*, *ALDH1L1*, *ALDOC*, *SLC1A2*, *AQP4*, *GFAP*, and *BLBP* relative to control human WM astrocytes (n = 4). **p* < 0.05. **(J)** The cleaved caspase 3 (CC3)-positive percentage of the 4,6-diamidino-2-phenylindole (DAPI)-positive cells was determined in oligodendrocyte cultures containing media conditioned by GM or WM astrocytes derived from control (n = 4) and VWM (n = 4) lines. Bars represent mean \pm standard error of the mean.

Discussion

In this study, we examined astrocyte subtype vulnerability in VWM. We generated functional astrocytes through differentiation protocols for control and VWM white and gray matter-like astrocyte subtypes from hiPSCs and miPSCs, using respectively CNTF or FBS supplementation. VWM astrocytes showed intrinsic defects. The WM astrocytes in both mouse and human models confirmed that specific astrocytic subtypes are more vulnerable for the VWM genotype. Pathways that were differentially regulated in VWM WM astrocytes involved immune system and extracellular matrix. Only in VWM patient models were changes in pathways related to neuronal functioning and vasculature identified. Cross-validation in different species models provided new insights into disease pathways in specific astrocyte subtypes in VWM, thereby helping development of new treatment strategies.

Astrocytes play a central role in pathology in VWM.^{8,11} The presented astrocytes derived from mouse and human iPSCs recapitulate earlier findings in mouse and human, such as increased proliferation, morphological abnormalities, and induction of decreased oligodendrocyte maturation.^{8,10} Interestingly, WM astrocytes are more vulnerable to VWM mutations than GM astrocytes, as indicated before in patient tissue.^{8,11} To our knowledge, we are the first to present VWM iPSC models involving subtype-specific astrocytes. Using mouse cultures, we demonstrated that WM astrocytes, but not GM astrocytes, inhibited oligodendrocyte maturation. This effect was not mediated via increased apoptosis of oligodendrocytes, as medium conditioned by VWM mouse WM astrocytes decreased the percentage of apoptotic cells compared to control astrocytes. This effect was not present in cultures containing medium conditioned by human WM astrocytes. This finding as well as other discrepancies between the mouse and human iPSC-based models may represent species-specific features. For example, earlier studies indicated that hyaluronic acid was immensely increased in brains of VWM patients, but only enhanced to some extent in severely affected VWM mice.¹⁷ Moreover, hyaluronic acid was not a clear determinant in disease phenotypes in primary cultures of VWM mouse cells.¹⁰ In the brain, hyaluronic acid is mainly produced by astrocytes and is known to inhibit oligodendrocyte maturation,²⁶ although a contribution of a neuronal and a oligodendrocyte component to elevated hyaluronic acid in the VWM patient brain cannot be excluded. Together, our findings show that iPSCs can be used to study intrinsic differences between astrocyte subtypes and to identify shared and unique disease mechanisms between species.

Transcriptome analyses on mouse and human iPSC cultures both suggest involvement of immune system and extracellular matrix in VWM pathology. In mouse cultures, only 13 DEGs between VWM and control were found, of which some genes have been related to VWM

disease mechanisms previously. *Cd44* encodes a transmembrane receptor that regulates cellular responses to hyaluronic acid, and was significantly upregulated in VWM compared to control mouse WM astrocytes. Previous studies showed an increase in CD44 expression in VWM patient white matter astrocytes in postmortem tissue.¹⁷ Furthermore, VWM mouse cultures showed decreased *Gli1* expression, which codes for a transcription factor that is a direct target of sonic hedgehog (SHH) signaling. SHH regulates proliferation of neural progenitor cells together with the intracellular receptor smoothed (SMO) and has neuroprotective effects.²⁷ Although not significant, *Sbh* and *Smo* levels were also decreased (2–2.5-fold) in VWM mouse WM astrocytes. A recent study showed an impaired SHH pathway in primary astrocytes from the *Eif2b5*^{R132H/R132H} mouse, confirming the involvement of the SHH pathway in VWM.²⁸ Interestingly, VWM mouse cultures also showed increased *Ets1* expression. *Ets1* is a transcription factor that is involved in the T-cell immune response and was shown to be upregulated in astrocytes surrounding white matter lesions in a mouse model for multiple sclerosis.²⁹ These findings suggest that the SHH pathway and immune response are interesting targets for VWM.

In addition to the pathways described for the mouse cultures, human WM astrocyte transcripts showed differences between VWM and controls that were associated with GO terms that we categorized as “Neuronal Functioning” and “Vasculature-Related.” The DEGs related to neuronal functioning include upregulation of *GRID1*, *GRIA2*, and *GRIN2A* in VWM, which encode subunits of membrane ionotropic N-methyl-D-aspartate and α -amino-3-hydroxy-5-methyl-4-isoxazolepropionic acid receptors. A downstream effect of activation of these receptors is stimulation of the adenosine triphosphate (ATP)-driven Na⁺ pump. This induces glycolytic upregulation of ATP and lactate in astrocytes, as well as regulation of the extracellular potassium concentration, because the ATP-driven Na⁺ pump actively pumps potassium into the cells.³⁰ The channel protein AQP4 is regulated by extracellular potassium levels and involved in water permeability of astrocytes, which can lead to neurotoxicity and myelin defects when dysregulated.³¹ Interestingly, VWM human WM astrocytes showed increased AQP4 levels. DEG analysis also included increased expression of *SLC6A1*, *SLC6A11*, and *GABBR2* in VWM, which encode major transmembrane γ -aminobutyric acid (GABA) transporters GAT-1, GAT-3, and GABA_B receptor subunit 2, respectively.³² Increased extracellular levels of GABA, released by interneurons for example, lead to astrocytic Ca²⁺ elevations mediated by GABA_B receptor activation. This may further lead to astrocytic glutamate release, thereby potentiating inhibitory synaptic transmission, and to astrocytic ATP/adenosine-mediated heterosynaptic suppression affecting excitatory transmission.³² This confirms earlier findings that neuronal dysfunction in VWM should not be overlooked.³³

Our human transcriptome data furthermore showed a number of DEGs involved in mitochondrial functioning, including *CTGF*, *CYP11B1*, *NTRK2*, *CNRI*, *TBX2*, and *MT2A*. *CNRI*, driven by *PAX3* expression,³⁴ both of which are upregulated in VWM human WM astrocytes, is known to regulate mitochondrial functioning and protects against neuroinflammation resulting from oxidative stress.^{35–37} *TBX2* was also upregulated in VWM human WM astrocytes. In astrocytoma cell lines, *TBX2* has been shown to promote proliferation, to inhibit cleaved caspase 3-mediated apoptosis by stimulating mitochondrial fission, and to increase mitochondrial DNA content.³⁸ In contrast to the protective effect of *TBX2*, our VWM human WM astrocytes also showed a decreased expression of *MT2A*, an antioxidative, anti-inflammatory, and anti-apoptotic metallothionein secreted by astrocytes that is well known for its neuroprotective properties.³⁹ Mitochondrial mechanisms involved in VWM pathophysiology corroborate recent findings in primary astrocytes of *Eif2b5*^{R132H/R132H} mice indicating that an impaired oxidative phosphorylation in these cells is compensated by increased mitochondrial content and glycolysis.²⁸ Thus, these pathways deserve further study to determine whether these can target for therapeutic strategies.

In conclusion, the transcript analysis confirmed pathways previously implicated in VWM, such as SHH and extracellular matrix-related proteins. Additionally, the immune system presented itself as a potential target. Interestingly, human specific signaling pathways that emerged suggested interaction with neuronal functioning and with the vasculature. Of note is the increased expression of various glutamate receptors as well as transmembrane GABA transporters. Finally, the finding of altered expression of a number of genes associated with mitochondrial functioning adds to recent insights in mitochondrial dysfunction in VWM pathology. Altogether, we have created new disease models for VWM using iPSC-derived white and gray matter-like astrocytes, and have demonstrated intrinsic vulnerability of the white matter-like subtypes in VWM. The use of the presented in vitro models may greatly aid further exploration of these new pathways possibly involved in VWM pathophysiology, and can be used in compound screening studies for drug development.

Acknowledgment

This research is funded by a ZonMw VIDI research grant (91712343, V.M.H.), a European Leukodystrophy Association research grant (2014-012L1, V.M.H.), an E-Rare Joint Call project (9003037601, V.M.H.), and an NWO Spinoza grant (M.S.v.d.K.).

We thank J. Broeke for his help with the calcium imaging of the astrocytes and A. Badia for her help with the morphological analysis using Columbus software.

Author Contributions

P.S.L., S.D., A.E.J.H., and V.M.H. contributed to conception and design of the study; P.S.L., S.D., A.E.J.H., K.W., G.J., P.C.-S. and L.G. contributed to the acquisition and analysis of data; P.S.L., S.D., A.E.J.H., M.S.v.d.K., and V.M.H. contributed to drafting the text and preparing the figures.

Potential Conflicts of Interest

Nothing to report.

References

1. Lundgaard I, Osorio MJ, Kress BT, et al. White matter astrocytes in health and disease. *Neuroscience* 2014;276:161–173.
2. Molofsky AV, Krencik R, Ullian EM, et al. Astrocytes and disease: a neurodevelopmental perspective. *Genes Dev* 2012;26:891–907.
3. Molofsky AV, Deneen B. Astrocyte development: a guide for the perplexed. *Glia* 2015;63:1320–1329.
4. Bayraktar OA, Fuentealba LC, Alvarez-Buylla A, Rowitch DH. Astrocyte development and heterogeneity. *Cold Spring Harb Perspect Biol* 2014;7:a020362.
5. Martinian L, Boer K, Middeldorp J, et al. Expression patterns of glial fibrillary acidic protein (GFAP)-delta in epilepsy-associated lesional pathologies. *Neuropathol Appl Neurobiol* 2009;35:394–405.
6. Yamanaka K, Komine O. The multi-dimensional roles of astrocytes in ALS. *Neurosci Res* 2018;126:31–38.
7. Middeldorp J, van den Berge SA, Aronica E, et al. Specific human astrocyte subtype revealed by affinity purified GFAP antibody; unpurified serum cross-reacts with neurofilament-L in Alzheimer. *PLoS One* 2009;4:e7663.
8. Bugiani M, Boor I, van Kollenburg B, et al. Defective glial maturation in vanishing white matter disease. *J Neuropathol Exp Neurol* 2011; 70:69–82.
9. Van der Knaap MS, Wolf NI, Heine VM. Leukodystrophies: five new things. *Neurol Clin Pract* 2016;6:506–514.
10. Dooves S, Bugiani M, Postma NL, et al. Astrocytes are central in the pathomechanisms of vanishing white matter. *J Clin Invest* 2016;126: 1512–1524.
11. Leferink PS, Breeuwsma N, Bugiani M, et al. Affected astrocytes in the spinal cord of the leukodystrophy vanishing white matter. *Glia* 2018;66:862–873.
12. Leung C, Jia Z. Mouse genetic models of human brain disorders. *Front Genet* 2016;7:40.
13. Chandrasekaran A, Avci HX, Leist M, et al. Astrocyte differentiation of human pluripotent stem cells: new tools for neurological disorder research. *Front Cell Neurosci* 2016;10:215.
14. Warlich E, Kuehle J, Cantz T, et al. Lentiviral vector design and imaging approaches to visualize the early stages of cellular reprogramming. *Mol Ther* 2011;19:782–789.
15. Nadadthur AG, Leferink PS, Holmes D, et al. Patterning factors during neural progenitor induction determine regional identity and differentiation potential in vitro. *Stem Cell Res* 2018;32:25–34.

16. Sloane JA, Batt C, Ma Y, et al. Hyaluronan blocks oligodendrocyte progenitor maturation and remyelination through TLR2. *Proc Natl Acad Sci U S A* 2010;107:11555–11560.
17. Bugiani M, Postma N, Polder E, et al. Hyaluronan accumulation and arrested oligodendrocyte progenitor maturation in vanishing white matter disease. *Brain* 2013;136(pt 1):209–222.
18. Shaltouki A, Peng J, Liu Q, et al. Efficient generation of astrocytes from human pluripotent stem cells in defined conditions. *Stem Cells* 2013;31:941–952.
19. Perriot S, Mathias A, Perriard G, et al. Human induced pluripotent stem cell-derived astrocytes are differentially activated by multiple sclerosis-associated cytokines. *Stem Cell Reports* 2018;11:1199–1210.
20. Dallner C, Woods AG, Deller T, et al. CNTF and CNTF receptor alpha are constitutively expressed by astrocytes in the mouse brain. *Glia* 2002;37:374–378.
21. Goursaud S, Kozlova EN, Maloteaux JM, Hermans E. Cultured astrocytes derived from corpus callosum or cortical grey matter show distinct glutamate handling properties. *J Neurochem* 2009;108:1442–1452.
22. Ishimoto T, Ninomiya K, Inoue R, et al. Mice lacking BCAS1, a novel myelin-associated protein, display hypomyelination, schizophrenia-like abnormal behaviors, and upregulation of inflammatory genes in the brain. *Glia* 2017;65:727–739.
23. Das PP, Hendrix DA, Apostolou E, et al. PRC2 is required to maintain expression of the maternal Gtl2-Rian-Mirg locus by preventing de novo DNA methylation in mouse embryonic stem cells. *Cell Rep* 2015;12:1456–1470.
24. Han Z, He H, Zhang F, et al. Spatiotemporal expression pattern of Mirg, an imprinted non-coding gene, during mouse embryogenesis. *J Mol Histol* 2012;43:1–8.
25. Dashzeveg N, Taira N, Lu ZG, et al. Palmdelphin, a novel target of p53 with Ser46 phosphorylation, controls cell death in response to DNA damage. *Cell Death Dis* 2014;5:e1221.
26. Back SA, Tuohy TM, Chen H, et al. Hyaluronan accumulates in demyelinated lesions and inhibits oligodendrocyte progenitor maturation. *Nat Med* 2005;11:966–972.
27. Patel SS, Tomar S, Sharma D, et al. Targeting sonic hedgehog signaling in neurological disorders. *Neurosci Biobehav Rev* 2017;74(pt A):76–97.
28. Atzmon A, Herrero M, Sharet-Eshed R, et al. Drug screening identifies sigma-1-receptor as a target for the therapy of WWM leukodystrophy. *Front Mol Neurosci* 2018;11:336.
29. Gerhauser I, Alldinger S, Baumgartner W. Ets-1 represents a pivotal transcription factor for viral clearance, inflammation, and demyelination in a mouse model of multiple sclerosis. *J Neuroimmunol* 2007;188:86–94.
30. Lanciotti A, Brignone MS, Bertini E, et al. Astrocytes: emerging stars in leukodystrophy pathogenesis. *Transl Neurosci* 2013;4(2).
31. Plog BA, Nedergaard M. The glymphatic system in central nervous system health and disease: past, present, and future. *Annu Rev Pathol* 2018;13:379–394.
32. Boddum K, Jensen TP, Magloire V, et al. Astrocytic GABA transporter activity modulates excitatory neurotransmission. *Nat Commun* 2016;7:13572.
33. Klok MD, Bugiani M, de Vries SI, et al. Axonal abnormalities in vanishing white matter. *Ann Clin Transl Neurol* 2018;5:429–444.
34. Marshall AD, Lagutina I, Grosveld GC. PAX3-FOXO1 induces cannabinoid receptor 1 to enhance cell invasion and metastasis. *Cancer Res* 2011;71:7471–7480.
35. Benard G, Massa F, Puente N, et al. Mitochondrial CB(1) receptors regulate neuronal energy metabolism. *Nat Neurosci* 2012;15:558–564.
36. Hebert-Chatelain E, Desprez T, Serrat R, et al. A cannabinoid link between mitochondria and memory. *Nature* 2016;539:555–559.
37. Esposito G, Izzo AA, Di Rosa M, Iuvone T. Selective cannabinoid CB1 receptor-mediated inhibition of inducible nitric oxide synthase protein expression in C6 rat glioma cells. *J Neurochem* 2001;78:835–841.
38. Yi F, Du J, Ni W, Liu W. Tbx2 confers poor prognosis in glioblastoma and promotes temozolomide resistance with change of mitochondrial dynamics. *Oncotargets Ther* 2017;10:1059–1069.
39. Ling XB, Wei HW, Wang J, et al. Mammalian metallothionein-2A and oxidative stress. *Int J Mol Sci* 2016;17(9).